Diverse Interactions between the Individual Mutations in a Double Mutant at the Active Site of Staphylococcal Nuclease†

David J. Weber,‡ Engin H. Serpersu,§ David Shortle, and Albert S. Mildvan*

Department of Biological Chemistry, The Johns Hopkins University School of Medicine, 725 N. Wolfe Street, Baltimore, Maryland 21205

Received April 18, 1990; Revised Manuscript Received June 4, 1990

ABSTRACT: In principle, the quantitative effect of a second mutation on a mutant enzyme may be antagonistic, absent, partially additive, additive, or synergistic with respect to the first mutation. Depending on the kinetic or thermodynamic parameter measured, the D21E and R87G mutations of staphylococcal nuclease exhibit four of these five categories of interaction in the double mutant. While V_{max} of the R87G single mutant of staphylococcal nuclease is $10^{4.8}$-fold lower than that of the wild-type enzyme and the V_{max} of the D21E single mutant is $10^{3.0}$-fold below that of wild type, the double mutant D21E + R87G was found to lose a factor of only $10^{4.1}$ in V_{max} relative to wild type, rather than the product of the two single mutations ($10^{7.8}$). These results suggest antagonistic structural effects of the individual R87G and D21E mutations. An alternative explanation for the nonadditivity of effects, namely, the separate functioning of these residues in a stepwise mechanism involving the prior attack of water on phosphorus followed by protonation of the leaving group by Arg-87, is unlikely since no enzyme-bound phosphorane intermediate (<1% of [enzyme]) was found under steady-state conditions on the R87G mutant by ^{31}P NMR at 242.9 MHz. Like the effects on V_{max}, quantitatively similar antagonistic effects of the two mutations were detected on the binding of divalent cations in binary enzyme–Ca^{2+} and enzyme–Mn^{2+} complexes and in the ternary enzyme–Ca^{2+}–5′-pdTdA complex, suggesting that the effects on V_{max} result from antagonistic structural changes at the Ca^{2+} binding site. Simple additive weakening effects of the two mutations were found on the binding of the substrate 5′-pdTdA, in both the absence and the presence of the divalent cations, Mn^{2+} and Ca^{2+}. However, synergistic effects of the two mutations were found on the binding of the substrate analogue 3′,5′-pdTp, profoundly weakening its binding to the double mutant in both the absence and the presence of divalent cations. Such synergistic effects of the two mutations may result from negative cooperativity or strain in the binding of 3′,5′-pdTp to the wild-type enzyme. It is concluded that the quantitative interactions of two active-site mutations of an enzyme can vary greatly depending on which parameter of the enzyme is measured. When the two mutations interact in the same way on several parameters, a common underlying mechanism is suggested.

Staphylococcal nuclease catalyzes the hydrolysis of phosphodiester linkages in both DNA and RNA to yield 3′-mononucleotides (Tucker et al., 1979; Mildvan & Serpersu, 1987). By comparing k_{cat} of this reaction with the pseudo-first-order rate constant for nonenzymic phosphodiester hydrolysis, extrapolated to the same temperature and pH, it has been estimated that staphylococcal nuclease accelerates this reaction by a factor of at least 10^{15}-fold or, more likely, 10^{16}-fold (Serpersu et al., 1987). A chemical mechanism based on the 1.5-Å X-ray structure of the ternary enzyme–Ca^{2+}–pdTp complex (Cotton et al., 1979; Loll & Lattman, 1989), extensive kinetic studies with intact and semisynthetic enzymes (Anfinsen et al., 1971; Chaiken & Sanchez, 1972), and kinetic and magnetic resonance studies of a large series of active site mutants (Serpersu et al., 1986, 1987, 1988a, 1989; Hibler et al., 1987) is shown in Figure 1. In this mechanism, the essential Ca^{2+} activator is bound in a septacoordinate complex (Loll & Lattman, 1989), receiving three cis ligands from Asp-21, Asp-40, and the amide carbonyl group of Thr-41, as well as one from a phosphodiester oxygen of the substrate. The attacking water molecule is postulated to be close enough to Glu-43 to permit its carboxylate group to function as a general base (Hibler et al., 1987; Serpersu et al., 1989). Upon nucleophilic attack, the phosphodiester of the substrate is converted to a trigonal-bipyrimidal transition state or intermediate, stabilized by Arg-87 (Serpersu et al., 1987), which also acts as a general acid to protonate the 5′-oxygen of the leaving nucleotide. The importance of Arg-87 to catalysis was shown by its mutation to Gly in the R87G mutant, which lowered k_{cat} by a factor $>10^{4.6}$ (Serpersu et al., 1987). Another mutant form of the enzyme, D21E, in which the Ca^{2+} ligand Asp-21 was enlarged to Glu, showed an unusually large $10^{3.2}$-fold decrease in k_{cat}, which may be due to overlap of the enlarged liganding residue with the binding site for the attacking water molecule (Serpersu et al., 1987) and to an increase in distance from the metal to the attacked phosphorus (Weber et al., 1990a), thus interfering with catalysis by approximation (Serpersu et al., 1987).

To further test these components of the reaction mechanism, the effects on the kinetic, metal-binding, and substrate-binding properties of staphylococcal nuclease were investigated in the double mutant D21E + R87G. Interestingly, depending on which parameter was studied, the effects of the individual mutations interacted differently in the double mutant. Pre-

† This work was supported in part by Grants DK28616 from the National Institutes of Health to A.S.M. and GM34171 to D.S.

* To whom correspondence should be addressed.

‡ National Institutes of Health Postdoctoral Fellowship (F32 GM 13324).

§ Present address: Department of Biochemistry, University of Tennessee, Knoxville, TN 37996.

0006-2960/90/0429-8632$02.50/0

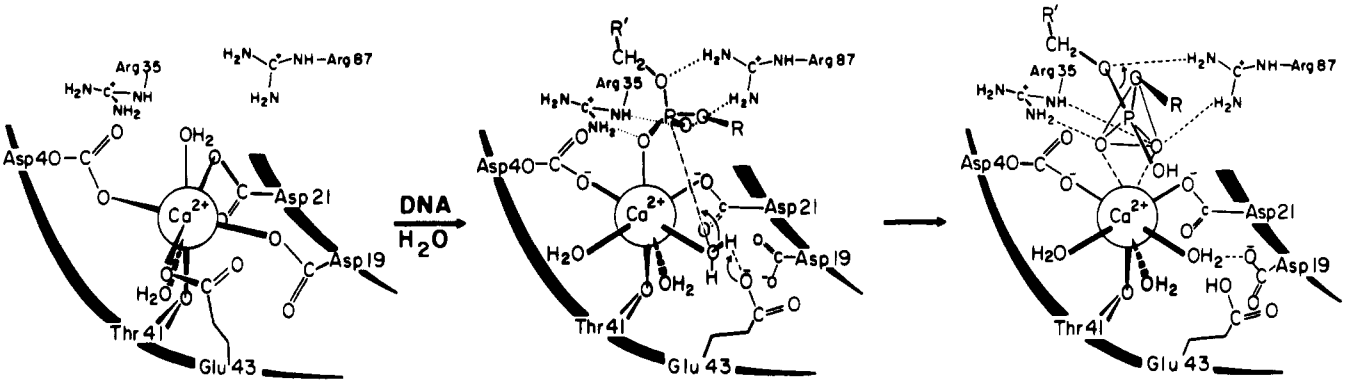

FIGURE 1: Mechanism of staphylococcal nuclease based on the 1.5-Å X-ray structure (Cotton et al., 1979), kinetic studies (Anfinsen et al., 1971), and studies of active-site mutants (Serpersu et al., 1987, 1988, 1989; Hibler et al., 1987) showing an additional water ligand on Ca^{2+}, as found in the refined X-ray structure (Loll & Lattman, 1989). Weak hydrogen bonding of the substrate by Arg-87 is shown, which is strengthened in the transition state.

liminary reports of this work have been published (Serpersu et al., 1988b; Weber et al., 1990b).

Experimental Procedures

Materials

The nucleotides 3′,5′-pdTp and 5′-pdTdA were obtained from P-L Biochemicals (Division of Pharmacia). Before use, buffer and nucleotide solutions were passed over Chelex 100 resin to remove trace metals. Highly polymerized salmon sperm DNA was purchased from Sigma, and all DNA used in the enzyme assays was denatured by boiling for 30 min followed by rapid cooling on ice and passed over Chelex 100 (Cuatrecasas et al., 1967a). Toluidine Blue (Sigma) was routinely filtered at 100 °C before use.

Methods

Isolation of Enzymes. The preparation, isolation, and sequence analysis of all single mutations in the staphylococcal nuclease gene were carried out as previously reported (Shortle & Lin, 1985). All mutant proteins are designated by their amino acid changes relative to the wild-type enzyme, using the three-symbol nomenclature in which the first letter designated the wild-type amino acid, the number designates the position of the amino acid, and the second letter designates the mutant amino acid substitution at that position. The double mutation was prepared by ligating *Ase*I restriction fragments from purified pF0G405 plasmids of the two single mutations D21E and R87G. The recombined DNA was identified by standard DNA sequencing methods (Shortle & Lin, 1985; Tabor & Richardson, 1987; Kunkel et al., 1987). Isolation of all mutant enzymes that carry the expression plasmid pF0G405 from the engineered strain of *Escherichia coli* was performed as described previously for the purification of wild-type enzyme (Serpersu et al., 1986).

Enzyme Assays. For highly active enzymes (i.e., wild type, D21E) the activity was measured by observing the absorbance increase at 260 nm as DNA is hydrolyzed (Cuatrecasas et al., 1967a,b). One unit of enzymatic activity is defined as the amount enzyme causing a change of 1.0 absorbance unit per minute at 260 nm in a 1-cm cell. Protein concentrations for all enzymes were determined by the absorbance at 280 nm ($\epsilon^{0.1\%} = 0.93$) at neutral pH (Dunn et al., 1973; Tucker et al., 1978, 1979). The assay mixture consisted of DNA (20–90 μg/mL), $CaCl_2$ (0.4–10.0 mM), and 40 mM Tris-HCl,[1] pH 7.4, in a volume of 1.0 mL at 24 °C. To start the reaction, enzyme (0.045–0.054 μg of wild type or 10.4–12.8 μg of D21E) was added. Velocity was determined from the linear portions of the recorder trace and expressed as the change in absorbancy per minute per microgram of protein. Enzymatic activities were linear with the amount of protein used in the assays. Analysis of the kinetic data for the wild-type and D21E mutant enzymes was carried out as described previously (Serpersu et al., 1987).

For mutants such as R87G and the double mutant D21E + R87G, with decreases in activity $\geq 10^4$ below that of the wild type enzyme, more sensitive assays were required. Two such assays were used. In the first, the nicking of supercoiled DNA was monitored by gel electrophoresis. Wild type (0.74–118 pM) and mutants of staphylococcal nuclease diluted with 0.5 mg/mL BSA were incubated in 20-μL solutions containing $CaCl_2$ (20.4 mM), pFOG 407, or actin plasmid DNA (25–200 μg/mL) and Tris-HCl (80 mM), pH 7.4, at 25 °C. All BSA stocks were Pentex grade (Miles Laboratories) and prepared by heating stock 5 mg/mL samples at 55 °C for 20 min. The nicking reaction was incubated for 12 min at 25 °C and stopped by the addition of 2 μL of a solution containing 500 mM EDTA, to give a final concentration of 45 mM. To test whether DNA was at saturating concentrations with the double-mutant enzyme, the nicking assay was performed at varying DNA concentrations (25–200 μg/mL) in the incubation mixtures. In all experiments, the DNA was precipitated by making the incubation mixture 0.4 M in sodium acetate and by a subsequent addition of 3 volumes of ethanol. The samples were stored at −20 °C for 3 h and centrifuged for 15 min in an Eppendorf microfuge (Model 5414). The pellet was dissolved in an appropriate amount of sample buffer (20 mM EDTA, 30% glycerol, 0.018% bromphenol blue, 40 mM Tris-HCl, pH 7.4) and then applied to an 0.9% agarose gel containing ethidium bromide. Quantitation was achieved by photographing the gel under ultraviolet radiation and scanning the negative with a scanning densitometer (Hoefer Scientific). The intensities of peaks arising from the remaining supercoiled DNA (Figure 2A, faster moving bands) and the nicked bands (Figure 2A, slower moving bands) were then measured by integration. The increase in amount of nicked DNA was plotted versus enzyme concentration for comparison of activities of mutant with wild-type enzyme (Figure 2B).

The second sensitive assay of staphylococcal nuclease, which gave nearly identical results, was based on the color change of a metachromatic dye from blue to pink upon the hydrolysis of DNA as the enzyme diffuses through a DNA-containing agar gel (Lachica et al., 1971; Shortle, 1983, 1986). This assay

[1] Abbreviations: Tris-HCl, tris(hydroxymethyl)aminomethane hydrochloride; BSA, bovine serum albumin.

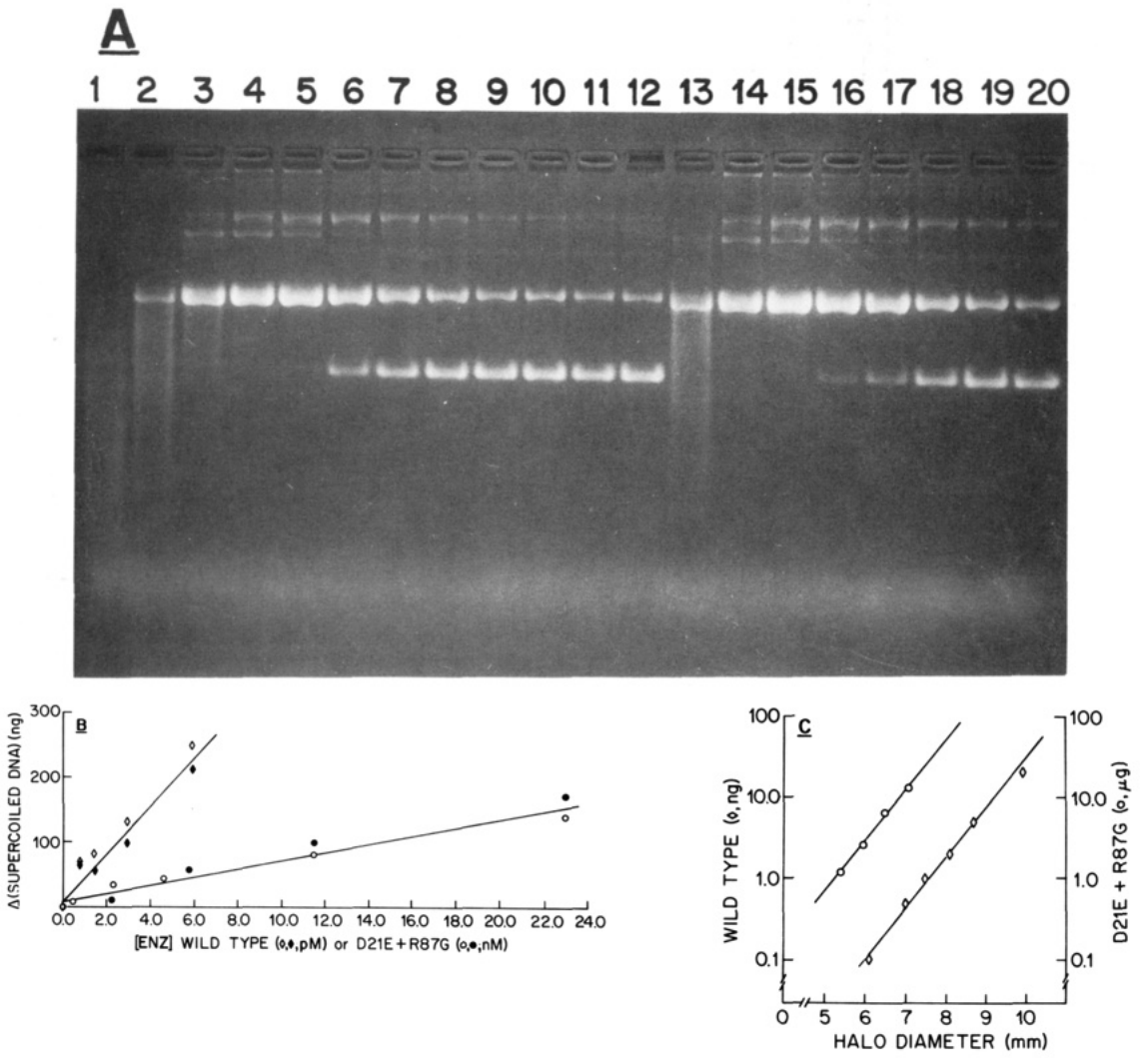

FIGURE 2: Kinetic studies of the D21E + R87G double mutant of staphylococcal nuclease in comparison with the wild-type enzyme. (A) Separation on agarose gel (0.9%) of nicked and supercoiled DNA plasmids (107.6 μg/mL) after a 12-min treatment with wild-type or D21E + R87G double-mutant staphylococcal nuclease. Concentrations (nM) of double-mutant enzyme in the assays were, lane 1, 2300; lane 2, 1150; lane 3, 459; lane 4, 230; lane 5, 144; lane 6, 45.9; lane 7, 23.0; lane 8, 11.5; lane 9, 4.60; lane 10, 2.30; lane 11, 0.458; and, lane 12, no enzyme. Concentrations (pM) of wild-type enzyme in the assays were, lane 13, 118; lane 14, 39.2; lane 15, 23.6; lane 16, 11.8; lane 17, 5.90; lane 18, 2.95; lane 19, 1.47; and, lane 20, 0.737. The fastest moving band is the substrate (supercoiled DNA). The band above that of the substrate is the product (nicked circular and linear DNA). At the highest enzyme concentrations (lanes 2 and 13) where further degradation of DNA to smaller linear fragments occurred, resulting in smearing, these data were not used for quantitation. (B) Amount of nicked DNA plasmid formed as a function of enzyme concentration, for comparing wild-type (◇, ◆) with double-mutant enzyme (○, ●). DNA concentrations in assays were 53.6 μg/mL (filled symbols) or 107.2 μg/mL (open symbols). Other components present were $CaCl_2$ (20.4 mM) and Tris-HCl, pH 7.4 (80 mM). Assay solutions were incubated for 12 min at 25 °C. (C) Quantitation of a single blue-plate assay according to Shortle (1983), showing log (total enzyme) applied to the blue plate in a 2-μL volume as a function of halo diameter for comparison of activities of wild-type (◇) with double-mutant enzyme (○). Conditions and components are given in Methods.

was also used to detect the low enzymatic activities of the R87G and D21E + R87G mutants relative to the wild-type enzyme, as previously described (Serpersu et al., 1987). Dilutions of the mutant enzymes over the range 1–12 μg were spotted in 2-μL volumes onto a Petri plate freshly prepared with 10 mL of agar gel containing 50 mM Tris-HCl, pH 7.4, 1% NaCl, 1% Difco agar, 300 μg/mL boiled salmon sperm DNA, 20 mM $CaCl_2$, and 0.2 mg/mL toluidine blue O. Plates were then incubated for 3 h at 30 °C, and the diameters of the pink halos formed in the blue plates by the diffusing active enzymes were measured with a transparent ruler. A standard curve for the wild-type enzyme was produced, and the amounts of wild-type enzyme (0.1–20 ng) were adjusted to give halos equal in diameter to those produced by the mutant enzymes, in order to compare relative activities (Figure 2C). The wild-type enzyme used as the standard for the comparisons in both assays had a specific activity of 2100–2700 units/mg in 40 mM sodium borate buffer, pH 8.8, utilizing the A_{260} spectrophotometric assay of Cuatrecasas et al. (1967a). Because of the high concentrations of DNA and Ca^{2+} used in this assay, saturation of the enzyme with these components was assumed and was supported by the agreement of the results of both assays.

Magnetic Resonance Measurements. The binding of Mn^{2+}, substrates, and substrate analogues to staphylococcal nuclease and its mutants was monitored by measuring the paramagnetic effects of Mn^{2+} on the longitudinal $(1/T_1)$ relaxation rate of water protons, measured with a Seimco pulsed NMR spectrometer at 24.3 MHz with a $180-\tau-90°$ pulse sequence as previously described (Carr & Purcell, 1954; Mildvan & Engle, 1972). The observed enhancement of relaxation rate is defined as $\epsilon^* = (1/T_{1P}^*)/(1/T_{1P})$, where $1/T_{1P}$ is the paramagnetic contribution to the relaxation rate in the presence (*) and absence of enzyme (Mildvan & Engle, 1972).

In independent Mn^{2+} binding studies, the concentration of free Mn^{2+} in a mixture of free and bound Mn^{2+} was deter-

mined by electron paramagnetic resonance (Cohn & Townsend, 1954) with a Varian E-4 EPR spectrometer. The NMR and EPR data were analyzed as previously described (Mildvan & Cohn, 1963, 1966; Mildvan & Engle, 1972; Serpersu et al., 1986, 1987) to determine the stoichiometry (n) of Mn^{2+} bound to each enzyme, the dissociation constant (K_D), and the enhancement factor (ϵ_b) of the binary enzyme–Mn^{2+} complex. In addition, the binding of Mn^{2+} to enzyme–3′,5′-pdTp and enzyme–5′-pdTdA complexes was monitored by EPR and by changes in $1/T_{1P}$* of water protons, providing independent measurements of the dissociation constants (K_A') of Mn^{2+} from ternary complexes. Titrations of the binary enzyme–Mn^{2+} complexes with 3′,5′-pdTp and 5′-pdTdA, monitoring changes in $1/T_{1P}$ of water protons, were analyzed by computer as previously described (Reed et al., 1970; Mildvan & Engle, 1972; Serpersu et al., 1987) to give dissociation constants (K_3) and enhancement factors (ϵ_T) of ternary complexes. The dissociation constants for binary and ternary Ca^{2+} complexes were obtained by competition experiments in which the corresponding Mn^{2+} complex was titrated with Ca^{2+}, monitoring the displacement of Mn^{2+} by the decrease in the enhancement (ϵ^*) of $1/T_{1P}$ of water protons, and independently by the appearance of free Mn^{2+} in the EPR spectrum.

^{31}P NMR Measurements. A search for an enzyme-bound phosphorane intermediate on the R87G mutant of staphylococcal nuclease was made by high-field ^{31}P NMR. ^{31}P NMR spectra were obtained at 242.9 MHz by using 12-bit analog to digital conversion collecting 16K or 32K data points with the maximum spectral width setting (50000 Hz) and acquisition times of 0.164 s and 0.328 s, respectively. Routine spectra were acquired in blocks of 1024 scans every 4.3 h over 24 h and then added to increase the signal to noise. For more frequent time points 8 or 64 scans were collected every 2.0 or 16.3 min, respectively. In all cases a 15.3-s recycle time was used to obtain fully relaxed spectra ($>5T_1$).

Samples (1.7 mL) contained 1.5 mM $(rC)_{18\pm6}$, 1.62 mM $p(dT)_8$, or poly(rC) (24.0 mM monomers) as well as 20% ^2H_2O for field/frequency locking, 1.0 mM EGTA, 110 mM KCl, and 100 mM Tris-HCl, pH 7.4. The R87G concentration was 1.10, 1.15, and 1.04 mM for the experiments with $(rC)_{18\pm6}$, $p(dT)_8$, and poly(rC), respectively. Spectra were acquired in the absence of Ca^{2+} and T_1 measurements using saturation recovery techniques were carried out to set the delay time. The reaction was then started by adding 1 M $CaCl_2$ (34 μL) (ultrapure ≥99.99%) to make the tube 20.0 mM in $CaCl_2$. All DNA and RNA samples were initially checked by NMR at 101.25 MHz for purity, before use. Preliminary time-course experiments were performed at 101.25 MHz with a 20000-Hz spectral width setting collecting 16K files with an acquisition time of 0.41 s. Spectra were acquired in these experiments in blocks of 512 scans every 2.2 h using a 15.4-s recycle time to ensure complete relaxation. In all experiments signals were referenced to external H_3PO_4 (85%).

Results

Kinetic Properties of the D21E + R87G Double Mutant and of the Individual Single Mutants of Staphylococcal Nuclease. The residual maximal enzymatic activity of the D21E + R87G double mutant, relative to that of the wild-type enzyme, was determined by sensitive assays measuring the extent of nicking of supercoiled DNA (Figure 2A,B) and the development of a halo due to DNA hydrolysis in an agar gel (Figure 2C) at varying enzyme concentrations. In the DNA nicking assay the appearance of product is linear with enzyme concentration (Figure 2A,B) and, at constant enzyme concentration, is linear with time for at least 15 min (not shown).

Table I: Factors of Decrease in V_{max} for Staphylococcal Nuclease Mutants Relative to That of Wild Type[a]

	assay			
mutant	DNA hydrolysis[b]	supercoil nicking[c]	blue plate[d]	average
R87G		$10^{-4.7}$	$10^{-4.8}$	$10^{-4.8\pm0.1}$
D21E	$10^{-3.2}$		$10^{-2.7}$	$10^{-3.0\pm0.2}$
D21E + R87G		$10^{-3.9}$	$10^{-4.3}$	$10^{-4.1\pm0.2}$

[a] Wild-type enzyme utilized in each assay was also assayed by DNA hydrolysis to give $0.714\Delta A/(\mu g\ min)$ at pH 7.4 at 24 °C, which can be expressed as k_{cat} = 95/s, assuming the molecular weight of the substrate to be that of an average tetranucleotide (MW = 1400) and ΔA = 0.3 for the complete hydrolysis of 50 μg/mL DNA (Cuatrecasas et al., 1967a,b; Serpersu et al., 1987). V_{max} for wild-type enzyme was arbitrarily assigned the value 1 for comparison. [b] The data are from Serpersu et al., 1987. [c] The dilutions of wild-type enzyme were adjusted to give bands of nicked DNA equal in amount to those produced by the mutant enzyme. [d] The dilutions of wild-type enzyme were adjusted to give pink halos equal in diameter to those produced by mutant enzyme.

As previously found (Shortle, 1983, 1986) the halo diameter, after a 3-h period of DNA hydrolysis, is a linear function of the logarithm of the total amount of active enzyme (Figure 2C). Maximal velocities were measured since the DNA nicking assays revealed no significant change in rates over a concentration range of DNA from 25 to 200 μg/mL, indicating saturation with DNA, and the halo assays were carried out at a DNA concentration of 300 μg/mL.

Table I compares the relative V_{max} values of the double-mutant enzyme with those of the individual single mutants. While V_{max} of the R87G mutant is $10^{4.8\pm0.1}$-fold lower than that of the wild-type enzyme and that of D21E is $10^{3.0\pm0.2}$-fold lower, V_{max} of the double mutant D21E + R87G is only $10^{4.1\pm0.2}$-fold below that of the wild-type enzyme.[2] Thus, the loss in maximal activity due to mutating both Arg-87 and Asp-21 is not the product of each individual effect ($10^{7.8}$) but is $10^{3.7}$-fold smaller than this product, such that the residual V_{max} of the double mutant is 5-fold greater than that of the more damaging single mutation R87G. In other words, the effects on V_{max} of the two single mutations D21E and R87G are antagonistic in the double mutant.

^{31}P NMR Studies of RNA and DNA Hydrolysis by the R87G Mutant Enzyme. Simple addition of the damaging effects of mutations of catalytic residues occurs when two residues act concertedly and independently in the same rate-limiting chemical step (Kuliopulos et al., 1990a,b; Xue et al., 1990). Since, in the present case, the product of the effects of the two single mutations on V_{max} was not observed in the double mutant, the possibility that Asp-21 and Arg-87 might function consecutively in a nonconcerted nucleophilic substitution at phosphorus was studied. This possibility must be considered because trigonal-bipyramidal phosphoranes may exist either as transition states or as true chemical intermediates (Mildvan & Fry, 1987). The R87G mutant enzyme was used since Arg-87 is believed to convert the phosphorane to the product by protonating the 5′-oxygen of the leaving nucleotide (Figure 1). The absence of Arg-87 might permit the accumulation of a phosphorane intermediate if such an intermediate existed. ^{31}P NMR spectra of a solution con-

[2] The DNase activity of these mutants is not likely to be due to contamination with other enzymes since several preparations of these mutants show the same residual activity, and, using the same preparative and assay methods, we have recently found lower activity of a different double mutant, E43S + R87G, which is $10^{5.7}$-fold below that of the wild-type enzyme.

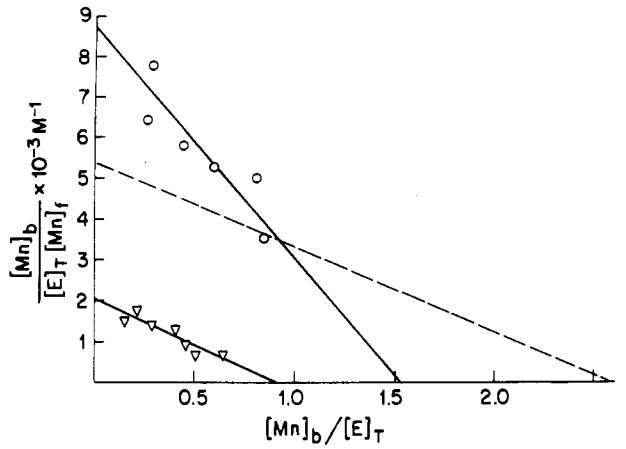

FIGURE 3: Scatchard plots of titrations of the D21E + R87G double mutant with Mn^{2+} in the absence (∇) or presence (○) of 3′,5′-pdTp, measuring the concentration of free Mn^{2+} by EPR. In the binary titration (∇) 508 μM enzyme was used. For the ternary titration 148 μM enzyme and 171 μM 3′,5′-pdTp were present. All solutions contained 40 mM Tris-HCl, pH 7.4. The dashed line shows the Scatchard plot calculated for the separate binding of Mn^{2+} to enzyme and pdTp with no ternary complex formation.

taining 1.15 mM enzyme and 1.62 mM $p(dT)_8$ were obtained in the absence of Ca^{2+} and at various times from 2 min to 24 h after starting the hydrolysis by the addition of 20 mM Ca^{2+}. Although hydrolysis was detected by the appearance of resonances at 4.62 ppm downfield from the external standard H_3PO_4, which increased in intensity with time, no phosphorane resonance (<1% of the enzyme) was observed between 0 and −90 ppm upfield of H_3PO_4 over a 24-h period of hydrolysis.

Similarly, in the presence of 1.04 mM enzyme, 20 mM $CaCl_2$, and poly(rC) (24 mM monomers) or 1.50 mM $(rC)_{18}$ no resonance upfield of H_3PO_4 was observed (<1% of the enzyme) although RNA hydrolysis was detected by the progressive appearance with time of narrow resonances at 4.62 ppm assigned to nucleoside 3′-phosphates. With RNA substrates, an additional signal appeared at 21.3 ppm downfield from H_3PO_4 assignable to 2′,3′-cyclic nucleotides probably due to trace contamination by a bacterial ribonuclease. Hence no evidence for a stepwise mechanism with a phosphorane intermediate was obtained.

Binary Mn^{2+} and Ca^{2+} Complexes of the D21E + R87G Double Mutant. To investigate the basis for the antagonistic effects of the mutations on V_{max} in the double mutant, metal and substrate binding studies were carried out. The binary enzyme–Mn^{2+} complex of the D21E + R87G double mutant was studied by direct titration of the enzyme with $MnCl_2$. At each point of the titration, the concentration of free Mn^{2+} was measured by EPR spectroscopy, and the enhancement (ϵ^*) of $1/T_{1P}$ of water protons, a function of the amount of bound Mn^{2+}, was determined by pulsed NMR. The values for free and bound Mn^{2+} determined by EPR spectroscopy were analyzed by a Scatchard plot (Figure 3) and compared to K_D^{Mn} values (Table II) previously determined for the wild-type, and R87G, and D21E single-mutant enzymes (Serpersu et al., 1986, 1987). The EPR data with three preparations of the double mutant D21E + R87G could be fit with a stoichiometry (n) of approximately one binding site for Mn^{2+} with a K_D^{Mn} = 412 ± 54 μM (Table II). Scatchard analysis of data from $1/T_{1P}$ of water protons yielded n and K_D^{Mn} values that showed good agreement with those measured by EPR on three preparations of the D21E + R87G double mutant (Table II). The K_D of Mn^{2+} from the double mutant is similar to the K_D values measured for both the wild-type enzyme (K_D = 438 μM) and the single, metal-liganding mutant D21E (K_D = 397 μM) but

Table II: Metal-Binding Properties of Binary Complexes of Mn^{2+} and Ca^{2+} and Enhancement of Mn^{2+} Mutant

enzyme or ligand	n	K_D^{Mn} or K_1^{Mn} (μM)	ϵ_b[d]	K_D^{Ca} or K_1^{Ca} (μM)
WT	0.95 ± 0.03[b] 1.00 ± 0.05[c]	11.0 ± 0.6 460 ± 63[c]	8.4 ± 0.7	510 ± 70[e]
D21E	0.94 ± 0.05[b] 0.95 ± 0.06[c]	396 ± 39[b] 398 ± 40[c]	6.2 ± 0.4	997 ± 103[e]
R87G	0.95 ± 0.05[b] 1.02 ± 0.06[c]	850 ± 83[b] 958 ± 93[c]	6.0 ± 0.2	4590 ± 280[e]
D21E + R87G	0.88 ± 0.06[b] 0.91 ± 0.08[c]	412 ± 54[b] 430 ± 50[c]	11.8 ± 0.9	666 ± 82[e]
3′,5′-pdTp	1.6 ± 0.2[b]	474 ± 50[b]	1.7 ± 0.1	1200 ± 700[f]
5′-pdTdA	1.0 ± 0.1[b]	2000 ± 200[b,c]	2.2 ● 0.1	7260 ± 800[e,f]

[a] n is constants of stoichiometry of and binding, K_D is the dissociation constant of the binary enzyme–metal complex, K_1 is are dissociation constant of the binary metal–nucleotide complex, and ϵ_b is the enhancement of the binary Mn^{2+} complex. The parameters for wild type, R87G, D21E, and 3′,5′-pdTp are from Serpersu et al. (1987). [b] Determined by EPR as in Figure 3. [c] Determined by $1/T_{1P}$ of water protons, using ϵ_b. [d] Determined by EPR and $1/T_{1P}$ of water protons. [e] Determined by competition with Mn^{2+} measuring $1/T_{1P}$ of water protons (Figure 4A). [f] Determined by competition with Mn^{2+} measuring free $[Mn^{2+}]$ by EPR (Serpersu et al., 1986).

2-fold lower than K_D of the R87G mutant (K_D = 904 μM) (Table II). The double mutant thus shows a 2-fold greater affinity for Mn^{2+} than found with the more damaging single mutation, R87G, indicating an antagonistic effect on Mn^{2+} binding of the D21E mutation on the R87G mutation. The enhancement factor of the double mutant (11.8 ± 0.9) slightly exceeds that of the wild-type enzyme (8.4 ± 0.7) but greatly exceeds those of the single mutants (6.1 ± 0.6), indicating a structural change in the coordination sphere of the bound metal.

The addition of Ca^{2+} to the binary Mn^{2+} complex of the double-mutant D21E + R87G enzyme decreased the observed enhancement, suggesting that Ca^{2+} displaces Mn^{2+} from the enzyme (Figure 4A). This point was established by EPR, which detected the appearance of free Mn^{2+}, and at high levels of Ca^{2+} essentially all of the Mn^{2+} was displaced. From the amount of Ca^{2+} required to displace half the bound Mn^{2+} and the measured dissociation constant of the binary enzyme–Mn^{2+} complex (Table II), a binary Ca^{2+}–enzyme dissociation constant (K_D^{Ca} = 666 ± 82 μM) was determined for the double mutant D21E + R87G. The value reported is an average dissociation constant determined from four titrations with two preparations of D21E + R87G. As found with Mn^{2+}, the affinity of the double mutant for Ca^{2+} in the binary complex is similar to the affinities measured for both the wild-type enzyme (K_D = 510 ± 70 μM) and the D21E metal liganding single mutant (K_D = 997 ± 103 μM) but is 6.9-fold tighter than that of the R87G mutant (K_D^{Ca} = 4590 ± 280 μM, Table II), indicating an antagonistic effect on Ca^{2+} binding of the D21E mutation on the R87G mutation.

Ternary Enzyme–Mn^{2+}–3′,5′-pdTp Complexes of the D21E + R87G Double Mutant. The thermodynamics of a ternary system of enzyme, metal, and nucleotide is described by six equilibrium constants, which are defined in Table III. The dissociation constant of the binary Mn^{2+} complex of the substrate analogue 3′,5′-pdTp (K_1) was previously determined (Serpersu et al., 1987) and those of the binary Mn^{2+}–enzyme complexes (K_D) were determined by EPR and PRR (Table II). To determine K_A', the dissociation constant of Mn^{2+} from the ternary enzyme–Mn^{2+}–nucleotide complex, the double mutant D21E + R87G, in the presence of an equivalent

Table III: Dissociation Constants (μM) and Enhancement Factors in Ternary Enzyme–Metal–3′,5′-pdTp Complexes of Wild-Type and Mutant Staphylococcal Nuclease[a]

complex	enzyme	K_A' EPR	K_A' $1/T_{1P}$[b]	$1/T_{1P}$ K_s[c,d]	$1/T_{1P}$ K_3[d]	$1/T_{1P}$ K_2[d]	$1/T_{1P}$ ϵ_T[d]
enzyme–Mn^{2+}–3′,5′-pdTp	WT	11.0 ± 0.6	17.0 ± 2.0	95 ± 30[e]	2.5 ± 1.0	2.2 ± 0.9	24.8 ± 0.4
	D21E	21.0 ± 1.6	20.3 ± 2.8	7.0 ± 1.6[e]	0.5 ± 0.2	0.42 ± 0.15	11.1 ± 1.2
	R87G	117 ± 9.0	175 ± 44	58 ± 17[e]	7.2 ± 1.9	13.0 ± 4.0	7.0 ± 0.8
	D21E + R87G	192 ± 32	215 ± 58	2980 ± 820[d]	1360 ± 370	1210 ± 373	20.2 ± 1.8
	enzyme		$K_A'^{Ca}$[e]	K_s^{Ca}	K_3^{Ca}[f]	K_2^{Ca}[g]	
enzyme–Ca^{2+}–3′,5′-pdTp	WT		71 ± 8	95 ± 30	13.1 ± 5.8	5.6 ± 1.9	
	D21E		184 ± 41	7.0 ± 1.6	1.7 ± 0.7	1.4 ± 0.8	
	R87G		1420 ± 380	58 ± 17	16.2 ± 5.9	62.1 ± 43	
	D21E + R87G		796 ± 294	2980 ± 820	3556 ± 1690	1977 ± 1290	

[a] The dissociation constants of the ternary and of the relevant binary complexes of enzyme (E), metal (M), and ligands (L) are defined as follows (Mildvan & Cohn, 1966): K_1 = [M][L]/[M–L]; K_D = [E][M]/[E–M]; K_2 = [E][M–L]/[E–M–L]; K_A' = [E–L][M]/[E–M–L]; K_3 = [E–M]-[L]/[E–M–L]; K_S = [E][L]/[E–L]. Note that $K_1K_2 = K_3K_D = K_A'K_S$. All parameters for wild type, D21E, and R87G are from Serpersu et al. (1987). [b] Determined by $1/T_{1P}$* of water protons in Mn^{2+} titrations. [c] Determined by Serpersu et al. (1987) utilizing an increase in fluorescence of 3′5′-ϵpAp when it was displaced by 3′,5′-pdTp and by computer analysis of nucleotide titrations. [d] Determined by computer analysis of nucleotide titrations (Figure 5) (Reed et al., 1970; Mildvan & Engle, 1972). [e] Determined by competition with Mn^{2+} measuring $1/T_{1P}$* of water protons (Figure 4A). [f] Based on $K_A'K_S/K_D$ (Tables II and III). [g] Based on $K_A'K_S/K_1$ (Tables II and III).

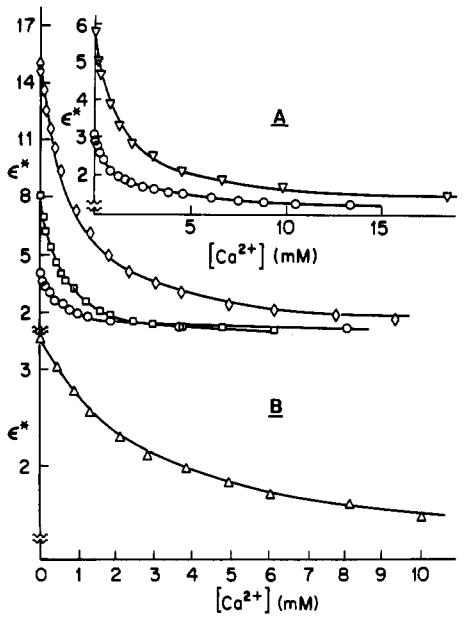

FIGURE 4: Displacement of Mn^{2+} by Ca^{2+} from various binary and ternary complexes of staphylococcal nuclease monitored by changes in the enhancement (ϵ^*) of the effects of Mn^{2+} on $1/T_1$ of water protons. (A) Displacement of Mn^{2+} by Ca^{2+} from binary (▽) and ternary enzyme–Mn^{2+}–3′,5′-pdTp complex (○) of the D21E + R87G double mutant. The solutions contained 508.2 μM D21E + R87G with 114.2 μM $MnCl_2$ (▽) and 163.4 μM D21E + R87G with 85.1 μM $MnCl_2$ and 180.4 μM 3′,5′-pdTp (○). (B) Displacement of Mn^{2+} by Ca^{2+} from ternary enzyme–Mn^{2+}–5′-pdTdA complexes of the wild type (◇), D21E (□), R87G (△), and D21E + R87G (○) enzymes. The solutions contained 65.3 μM wild-type enzyme with 65.3 μM $MnCl_2$ and 86 μM 5′-pdTdA (◇), 49.7 μM D21E mutant with 26.3 μM $MnCl_2$ and 52.7 μM 5′-pdTdA (□), 169.6 μM R87G mutant with 152.4 μM $MnCl_2$ and 172.0 μM 5′-pdTdA (△) or 164.4 μM D21E + R87G double mutant with 96.0 μM $MnCl_2$ and 162.5 μM 5′-pdTdA (○). All solutions contained 40 mM Tris-HCl, pH 7.4. For all titrations Ca^{2+} was added from concentrated stock solutions that also had the other components of the titration at the same final concentrations. In both (A) and (B) the data points are shown together with best-fit K_{app} curves (Surpersu et al., 1986).

amount of 3′,5′-pdTp, was titrated with Mn^{2+}, measuring the free Mn^{2+} by EPR and independently the effects of bound Mn^{2+} on the $1/T_1$ of water protons.

Average dissociation constants derived from Scatchard plots of the EPR (Figure 3) and the $1/T_{1P}$ data indicate that the dissociation constant of Mn^{2+} from the ternary 3′,5′-pdTp complex of the double mutant (K_A' = 204 ± 58 μM) is

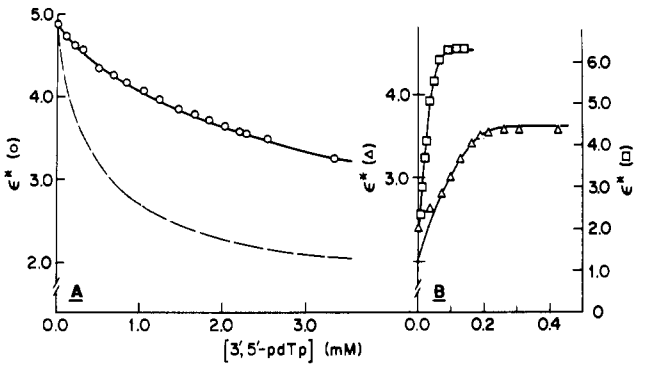

FIGURE 5: Titrations of Mn^{2+} complexes of single and double mutants of staphylococcal nuclease with 3′,5′-pdTp, measuring the changes in the enhancement ϵ^* of the paramagnetic effects of Mn^{2+} on $1/T_1$ of water protons. (A) Binding of the nucleotide 3′,5′-pdTp to the double mutant–Mn^{2+} binary complex. The solution contained 274 μM D21E + R87G and 98.5 μM Mn^{2+} (○). The dashed line represents a theoretical curve if pdTp only removed Mn^{2+} from the enzyme and no ternary complex was formed. (B) The binding of the nucleotide 3′,5′-pdTp to the single mutants R87G–Mn^{2+} (△) and D21E–Mn^{2+} (□) complexes (Serpersu et al., 1987) is displayed for comparison with the double-mutant titration. The nucleotide was added from concentrated stock solutions, which also contained all other components of the titration at the same concentrations. Solid curves are computed, using the parameters given in Tables II and III.

14.6-fold greater than that of the wild-type enzyme (14 ± 3.0 μM) (Table III). This factor is comparable to the product of the effects of the individual single mutations since K_A' of the D21E mutant is 1.5-fold greater than that of the wild-type enzyme and K_A' of the R87G mutant is 10.4-fold greater (Table III), suggesting additive effects of the two mutations on the ΔG of Mn^{2+} binding. The weakness of the resulting ternary complex may be seen by comparing the average K_A' and K_D values (Tables II and III) which indicates that 3′,5′-pdTp tightens the binding of Mn^{2+} to the double mutant D21E + R87G by a factor of only 2.2. The presence of 3′,5′-pdTp was previously shown to raise the affinity of the wild type and single-mutant enzymes D21E and R87G for Mn^{2+} by larger factors of 31, 18.9, and 6.2, respectively (Serpersu et al., 1987).

Further evidence for an unusually weak ternary 3′,5′-pdTp complex of the double mutant was obtained by determining K_3, the dissociation constant of the nucleotide from the ternary enzyme–Mn^{2+}–3′,5′-pdTp complex. Titrations of solutions of enzyme and Mn^{2+} with 3′,5′-pdTp, measuring changes in the enhancement (ϵ^*) of $1/T_{1P}$ of water protons (Mildvan &

Table IV: Dissociation Constants (μM) and Enhancement Factors in Ternary Enzyme–Metal–5′-pdTdA Complexes of Wild-Type and Mutant Staphylococcal Nuclease[a]

complex	enzyme	K_A' EPR	K_A' $1/T_{1P}$[b]	$1/T_{1P}$ K_S[c]	K_3[c]	K_2[c]	ϵ_T[c]
E–Mn^{2+}–5′-pdTdA	WT	6.3 ± 0.1	6.3 ± 0.1	44.7 ± 1.1	0.667 ± 0.02	0.14 ± 0.01	21.8 ± 0.8
	D21E	20.7 ± 2.0	21.3 ± 4.3	51.8 ± 5.3	2.74 ± 0.2	0.55 ± 0.10	12.2 ± 0.6
	R87G	382 ± 40	275 ± 54	233 ± 63	71.8 ± 18	32.4 ± 8.0	10.7 ± 0.5
	D21E + R87G	289 ± 25	301 ± 37	606 ± 200	344 ± 100	72.6 ± 22.0	11.6 ± 0.6
	enzyme		$K_A'^{Ca}$[d]	K_S^{Ca}	K_3^{Ca}[e]	K_2^{Ca}[f]	
E–Ca^{2+}–5′-pdTdA	WT		63.4 ± 6	44.7 ± 1.1	5.56 ± 0.60	0.390 ± 0.050	
	D21E		180 ± 28	51.8 ± 5.3	9.36 ± 1.43	1.29 ± 0.20	
	R87G		1830 ± 290	233 ± 63	93 ± 25	58.7 ± 16.0	
	D21E + R87G		343 ± 39	606 ± 200	312 ± 95	28.6 ± 7.7	

[a] The dissociation constants of the ternary and relevant binary complexes of enzyme, metal, and ligands are defined in Table III. [b] Determined by $1/T_{1P}$* of water protons in Mn^{2+} titrations. [c] Determined by computer analysis of nucleotide titrations (Figure 7) (Reed et al., 1970; Mildvan & Engle, 1972). [d] Determined by competition with Mn^{2+} measuring $1/T_{1P}$* of water protons (Figure 4B). [e] Based on $K_A'K_S/K_D$ (Tables II and IV). [f] Based on $K_A'K_S/K_1$ (Tables II and IV).

Engle, 1972) were fit by computed curves exemplified in Figure 5A, to yield the average K_3 values given in Table III. Unlike the wild-type and both single-mutant enzymes, a reduction in ϵ* occurred upon the addition of 3′,5′-pdTp to the double mutant (Figure 5). This decrease in ϵ* is, however, not as large as that calculated by assuming the simple removal of Mn^{2+} by 3′,5′-pdTp due to the formation of the two binary complexes (Figure 5A; dashed line). A very weak ternary complex was detected with a dissociation constant K_3 that is 544-fold greater than that of the wild-type enzyme (Table III). Since the single mutants R87G and D21E show much smaller effects on K_3 of 2.9- and 0.2-fold, respectively, the D21E mutation has synergistically weakened the binding of pdTp to the R87G–Mn^{2+} complex.

The computer fitting of the nucleotide titrations required values for K_S, the dissociation constant of the binary enzyme–nucleotide complex. Although determined indirectly by such analyses, the resulting K_S value (2980 ± 820 μM, Table III) was consistent with the data from six nucleotide titrations at four Mn^{2+} concentrations, ranging from 73.9 to 130 μM, and at a constant enzyme concentration (274 μM). The K_S for the 3′,5′-pdTp complex with the double mutant is far greater than the K_S for the wild-type enzyme (95 ± 30 μM) or either of the single mutants R87G (58 ± 17 μM) or D21E (7.0 ± 1.6 μM) (Table III), indicating that the combined effects of the double mutant profoundly weaken the binding of pdTp to the enzyme by a synergistic effect not detected in either of the single mutants.

Ternary Ca^{2+} Complexes of Wild-Type and Mutant Enzyme with 3′,5′-pdTp. Titrations of ternary enzyme–Mn^{2+}–nucleotide complexes with Ca^{2+} were carried out by measuring the decrease in $1/T_{1P}$ of water protons (Figure 4A) resulting from the displacement of the Mn^{2+} by Ca^{2+}, as independently observed by EPR. The results of four such titrations with three preparations of the double mutant gave dissociation constants (K_A') of Ca^{2+} from the ternary enzyme–Ca^{2+}–3′,5′-pdTp complex, which are compared in Table III with those previously obtained, under identical conditions, with the wild type and with both single mutants (Serpersu et al., 1987). Unlike the findings with Mn^{2+} where the effects of the single mutations on K_A' were additive, the weakening effects of the single mutations on K_A' of Ca^{2+} interact antagonistically in the double mutant. Thus, the R87G and D21E single mutations increased the K_A' of Ca^{2+} by factors of 20 ± 6 and 2.6 ± 0.6, respectively, while the double mutation increased K_A' by a factor of 11.2 ± 4.3. Stated another way, the K_A' of Ca^{2+} in the D21E + R87G double mutant is 1.8-fold tighter than that of the R87G single mutant and 4.3-fold weaker than that of the D21E single mutant.

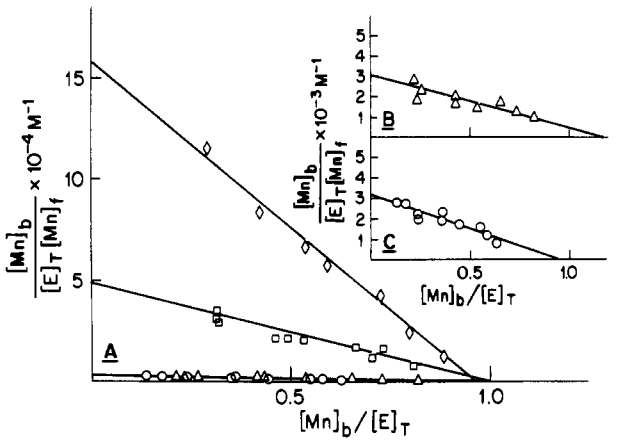

FIGURE 6: Scatchard plots of titrations of wild-type and mutant enzymes with Mn^{2+} in the presence of 5′-pdTdA. (A) The solutions contained 59 μM wild-type enzyme and 86 μM 5′-pdTdA (◇), 40.3 μM D21E and 43.0 μM 5′-pdTdA (□), 169 μM R87G and 172 μM 5′-pdTdA (△), and 164 μM D21E + R87G and 163 μM 5′-pdTdA (○) in 40 mM Tris-HCl, pH 7.4. (B) The data for the R87G mutant (△) and (C) for the D21E + R87G mutant (○) are replotted in expanded form. A plot based on $1/T_{1P}$ data is shown for the wild-type enzyme and on EPR data for all other enzymes.

These $K_A'^{Ca}$ values, together with the K_D^{Ca} values (Table II) and the K_S values (Table III) yielded K_3 values for the ternary Ca^{2+} complexes from the relationship $K_3 = K_A'K_S/K_D$ (Table III). For the double mutant the dissociation constant K_3 of 3′,5′-pdTp from the ternary enzyme–Ca^{2+}–3′,5′-pdTp complex (3556 μM, Table III) is 2–3 orders of magnitude greater than K_3 of wild-type enzyme or either single mutant. The profound weakening of pdTp binding noted in the estimate of K_S is thus reflected in K_3 as well; i.e. the binding of Ca^{2+} has no significant tightening effect on the binding of pdTp to the double mutant (Table III). In contrast, comparisons of K_3 with K_S (Table III) reveal that Ca^{2+} significantly raises the affinity of the wild-type enzyme and the D21E and R87G single mutants for 3′,5′-pdTp.

Ternary Mn^{2+} Complexes of Wild-Type and Mutant Enzymes with 5′-pdTdA. Because of the very weak ternary complexes formed by the D21E + R87G double mutant with the substrate analogue 3′,5′-pdTp ternary complexes of the dinucleotide substrate 5′-pdTdA, a larger ligand, were studied by utilizing the same methodology. From Scatchard plots of Mn^{2+} titrations exemplified in Figure 6, K_A' of Mn^{2+} from the ternary enzyme–Mn^{2+}–5′-pdTdA complex of the double mutant (295 ± 25 μM) was found to be 47-fold greater than that

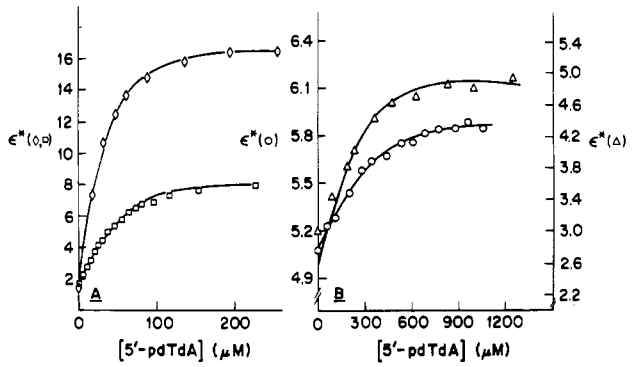

FIGURE 7: Titrations of Mn^{2+} complexes of the wild-type, R87G, D21E, and D21E + R87G enzymes with 5'-pdTdA, measuring the changes in enhancement (ϵ^*) of the paramagnetic effects of Mn^{2+} on the $1/T_1$ of water protons. (A) Titration of Mn^{2+} complexes of the wild type (◇) and D21E mutant (□) with 5'-pdTdA. The solutions contained 59.1 μM wild type with 45.2 μM $MnCl_2$ or 53.6 μM D21E and 50.3 μM $MnCl_2$ and 40 mM Tris-HCl, pH 7.4. (B) Titration of Mn^{2+} complexes of R87G (△) and D21E + R87G double mutant (○) with 5'-pdTdA. The solutions contained 254.4 μM R87G and 96.3 μM $MnCl_2$ or 274 μM D21E + R87G and 51.8 μM $MnCl_2$ and 40 mM Tris-HCl, pH 7.4. Nucleotides were added from concentrated stock solutions, which also contained all other components of the titration at the same final concentrations. The data points are shown, together with curves computed by using the parameters given in Tables II and IV.

of the wild-type enzyme (6.3 ± 0.1 μM) and indistinguishable from K_A' for the single mutant R87G (328 ± 54 μM) (Table IV). Hence the D21E mutation, which by itself weakens K_A' by a factor of 3.3, has had no additional weakening effect on K_A' in the double mutant beyond that produced by the R87G mutation. By comparing K_A' and K_D values it is found that 5'-pdTdA tightens the binding of Mn^{2+} to the double mutant 1.4-fold (Tables II and IV). With the wild-type, D21E, and R87G enzymes, 5'-pdTdA is found to raise the affinity for Mn^{2+} by larger factors of 69, 19.4, and 2.8, respectively, establishing the formation of ternary complexes in all cases.

Unlike the findings with the substrate analogue pdTp, in titration of the double mutant and Mn^{2+} with 5'-pdTdA, the observed enhancement (ϵ^*) of $1/T_{1P}$ increased due to the increased binding of Mn^{2+} by the enzyme. Such titrations were fit by computed curves (Figure 7) to yield K_3, the dissociation constant of 5'-pdTdA from the ternary complex of the double mutant. Similar increases of ϵ^* were observed with the wild-type and the individual single mutant enzymes (Figure 7), the parameters of which are also given in Table IV.

In the ternary enzyme–Mn^{2+}–5'-pdTdA complexes the effects of the single mutations on K_3 are additive in the double mutant. Thus, K_3 of the D21E mutant is 4.1-fold greater than that of the wild type and K_3 of the R87G mutant is 108-fold greater, while K_3 of the double mutant is (516 ± 150)-fold greater, which agrees within error with the product of the effects of the two single mutations (443 ± 116) (Table IV). Similarly, the weakening effects of the two single mutations on K_S, the dissociation constant of the binary enzyme–5'-pdTdA complex, are also approximately additive in the double mutant (Table IV). Thus K_S of the D21E mutant is (1.2 ± 0.1)-fold greater than that of the wild-type enzyme and K_S of the R87G mutant is 5.2 ± 1.4-fold greater, while that of the double mutant is (13.6 ± 4.5)-fold greater, which is comparable to the product of the effects of the two single mutations (6.2 ± 2.0).

Larger K_3 and K_S values, indicating weaker nucleotide binding by the R87G mutant, compared with the wild-type enzyme, were observed with the substrate 5'-pdTdA (Table IV) but not with the substrate analogue 3',5'-pdTp (Table III, Serpersu et al., 1987) suggesting some hydrogen bonding of Arg-87 to the enzyme-bound substrate in the ground state (Figure 1).

Ternary Ca^{2+} Complexes of Wild-Type and Mutant Enzymes with 5'-pdTdA. The dissociation constant of Ca^{2+} from the ternary enzyme–Ca^{2+}–5'-pdTdA complexes of the wild-type and mutant enzymes, K_A', was found to be measurable by Mn^{2+} displacement titrations (Figure 4B) before significant amounts of hydrolysis of 5'-pdTdA occurred (<5%) as detected by thin-layer chromatography. While the single mutations R87G and D21E both increased K_A' by factors of 28.9 and 2.9, respectively, over that of the wild-type enzyme, the double mutant D21E + R87G showed only a 5.4-fold increase in K_A' (Table IV). Thus the D21E mutation antagonized the effect of the R87G mutation on Ca^{2+} binding in the ternary enzyme–Ca^{2+}–5'-pdTdA complex, by a factor of 5.3.

As found with the Mn^{2+} complexes, the dissociation constant K_3 of the dinucleotide 5'-pdTdA from the ternary Ca^{2+} complex of the double mutant showed approximately additive effects of the two single mutations. Thus, the D21E + R87G double mutant showed a (56 ± 18)-fold increase in K_3 over that of the wild-type enzyme, comparable to the product (28 ± 10) of the effects of the D21E and R87G single mutations, which increased K_3 by factors of 1.7 ± 0.3 and 16.7 ± 4.8, respectively (Table IV). The weakening of substrate binding by the R87G mutation suggests weak hydrogen bonding of Arg-87 to the enzyme-bound substrate in the active ternary complex.

Discussion

The quantitative effects of mutations on kinetic and thermodynamic parameters of enzymes are most conveniently expressed as changes in free energy of activation (ΔG^*) and binding (ΔG), respectively, compared to those of the wild-type enzyme. Consider two mutations, 1 and 2, which affect a parameter of the wild-type enzyme by ΔG_1 and ΔG_2, respectively, when acting separately, and by ΔG_{1+2} in a double mutant. Assume that mutation 1 alone is more damaging than mutation 2 alone, i.e., $\Delta G_1 > \Delta G_2$. In principle, the quantitative effect of the second mutation (ΔG_2) on a parameter of the more damaging first mutation (ΔG_1) in the double mutant (ΔG_{1+2}) could be antagonistic ($\Delta G_{1+2} < \Delta G_1$), none ($\Delta G_{1+2} = \Delta G_1$), partially additive ($\Delta G_1 < \Delta G_{1+2} < \Delta G_1 + \Delta G_2$), additive ($\Delta G_{1+2} = \Delta G_1 + \Delta G_2$), or synergistic ($\Delta G_{1+2} > \Delta G_1 + \Delta G_2$). As summarized in Table V, one may determine the appropriate category for a given pair of mutations by analyzing the two free energy differences $\Delta\Delta G_A = \Delta G_{1+2} - \Delta G_1$ and $\Delta\Delta G_B = \Delta G_{1+2} - \Delta G_1 - \Delta G_2$. The former, $\Delta\Delta G_A$, measures the effect of the second mutation on the more damaging first mutation in the double mutant and is independent of ΔG_2, the effect of the second mutation alone, and of the parameters of the wild-type enzyme, which cancel. $\Delta\Delta G_A$ is negative in sign for antagonistic effects, zero for no additional effect, and positive for all other categories. These other categories may be distinguished by comparing $\Delta\Delta G_A$ with ΔG_2. $\Delta\Delta G_A$ thus measures the departure from no additional effect of the second mutation on the first and is widely used.

The second free energy difference, $\Delta\Delta G_B$, is the difference between the effect of the double mutation and the sum of the effects of both single mutations on the wild-type enzyme and measures the departure from simple additivity of the effects of the two mutations on the wild-type enzyme, i.e., the interaction energy of the two mutations in the wild-type enzyme. It is positive in sign for synergistic effects, zero for additive effects, and negative for all other categories. These other

Table V: Categories of Interaction of the Effects of Two Mutations on the Kinetic and Thermodynamic Parameters of an Enzyme

effect of second mutation on first[a]	definition	$\Delta\Delta G_A$[b]	$\Delta\Delta G_B$[c]	possible mechanisms[d]
antagonistic (suppressive)	$\Delta G_{1+2} < \Delta G_1$	<0	$<-\Delta G_2$	opposing structural effects on the same step
none	$\Delta G_{1+2} = \Delta G_1$	0	$-\Delta G_2$	opposing structural effects on the same step (limiting case); cooperatively interacting residues facilitating the same step (limiting case); effects on separate steps
partially additive	$\Delta G_1 < \Delta G_{1+2} < \Delta G_1 + \Delta G_2$	$0 < \Delta\Delta G_A < \Delta G_2$	$-\Delta G_2 < \Delta\Delta G_B < 0$	cooperatively interacting residues facilitating the same step[d]
additive	$\Delta G_{1+2} = \Delta G_1 + \Delta G_2$	ΔG_2	0	noninteracting residues facilitating the same step
synergistic	$\Delta G_{1+2} > \Delta G_1 + \Delta G_2$	$>\Delta G_2$	>0	anticooperatively interacting residues facilitating the same step; extensive unfolding of enzyme[d]

[a] Effect of less damaging mutation (ΔG_2) on more damaging mutation (ΔG_1) measured in double mutant (ΔG_{1+2}), where ΔG_n is the free energy difference between a parameter of the indicated mutant and that of the wild-type enzyme. By definition $\Delta G_1 > \Delta G_2$. For rate constants, free energies of activation ($\Delta G^{\ddagger}$) are meant. [b] The difference in free energy $\Delta\Delta G_A = \Delta G_{1+2} - \Delta G_1$ measures the effect of the less damaging mutation (ΔG_2) on the more damaging mutation (ΔG_1) in the double mutant (ΔG_{1+2}), i.e., the departure from no effect. Note that if the opposite convention were used, namely, the effect of the more damaging mutation (ΔG_1) on the less damaging mutation (ΔG_2) in the double mutant (ΔG_{1+2}), categories may change. Thus antagonistic effects may become either "none" or partially additive and "none" may become partially additive. [c] The difference in free energy $\Delta\Delta G_B = \Delta G_{1+2} - \Delta G_1 - \Delta G_2$ measures the departure from simple additivity, i.e., the interaction energy of the two mutations in the wild-type enzyme. The categories defined by $\Delta\Delta G_B$ do not depend on the relative magnitudes of ΔG_1 and ΔG_2 provided that both are positive. [d] Additional possible explanations can be shown, mathematically, to exist. For example, *synergistic* effects on k_{cat} of two mutations can occur if both affect the rate of the same step, which is not rate limiting in the wild-type enzyme but becomes more rate limiting in the double mutant. *Partially additive* effects on k_{cat} of two mutations can occur if each single mutation affects the rate of consecutive steps that are not rate limiting (Kuliopulos et al., 1990b).

Table VI: Changes in Free Energy of Activation and Binding (kcal/mol) by Staphylococcal Nuclease Resulting from the D21E, R87G, and D21E + R87G Mutations[a]

effect of S_1 on S_2	parameter	ΔG_1	ΔG_2	ΔG_{1+2}	$\Delta\Delta G_A$[b]	$\Delta\Delta G_B$[c]
antagonistic	V_{max}	6.5 ± 0.1	4.1 ± 0.3	5.6 ± 0.3	−0.9 ± 0.3	−5.0 ± 0.4
	K_D(Ca)	1.3 ± 0.1	0.4 ± 0.1	0.2 ± 0.1	−1.1 ± 0.2	−1.5 ± 0.2
	K_A'(Ca,pdTdA)	2.0 ± 0.2	0.6 ± 0.1	1.0 ± 0.1	−1.0 ± 0.2	−1.6 ± 0.2
	K_D(Mn)	0.43 ± 0.06	−0.06 ± 0.03	−0.02 ± 0.01	−0.5 ± 0.1	−0.4 ± 0.1
none	K_2(Ca,pdTdA)	2.9 ± 0.2	0.7 ± 0.2	2.5 ± 0.2	−0.4 ± 0.4	−1.1 ± 0.6
	K_A'(Ca,pdTp)	1.7 ± 0.2	0.6 ± 0.2	1.4 ± 0.2	−0.3 ± 0.3	−0.9 ± 0.4
	K_A'(Mn,pdTdA)	2.3 ± 0.1	0.7 ± 0.01	2.2 ± 0.1	−0.1 ± 0.1	−0.8 ± 0.1
partially additive						
additive	K_S(pdTdA)	0.97 ± 0.20	0.09 ± 0.07	1.53 ± 0.25	0.6 ± 0.4	0.5 ± 0.5
	K_A'(Mn,pdTp)	1.4 ± 0.2	0.2 ± 0.2	1.6 ± 0.2	0.2 ± 0.3	0.0 ± 0.3
	K_3(Mn,pdTdA)	2.7 ± 0.2	0.8 ± 0.1	3.6 ± 0.2	0.9 ± 0.2	0.1 ± 0.2
	K_3(Ca,pdTdA)	1.7 ± 0.2	0.3 ± 0.1	2.4 ± 0.2	0.7 ± 0.3	0.4 ± 0.4
	K_2(Mn,pdTdA)	3.2 ± 0.2	0.8 ± 0.1	3.7 ± 0.2	0.5 ± 0.3	−0.3 ± 0.3
synergistic	K_S(pdTp)	−0.3 ± 0.4	−1.5 ± 0.3	2.0 ± 0.4	2.3 ± 0.5	3.8 ± 0.6
	K_3(Mn,pdTp)	0.6 ± 0.4	−0.9 ± 0.5	3.7 ± 0.4	3.1 ± 0.6	4.0 ± 0.8
	K_3(Ca,pdTp)	0.1 ± 0.5	−1.2 ± 0.5	3.3 ± 0.6	3.2 ± 0.8	4.4 ± 0.9
	K_2(Mn,pdTp)	1.0 ± 0.5	−1.0 ± 0.5	3.7 ± 0.5	2.7 ± 0.7	3.7 ± 0.8
	K_2(Ca,pdTp)	1.4 ± 0.6	−0.8 ± 0.7	3.4 ± 0.5	2.0 ± 0.8	2.8 ± 1.0

[a] ΔG_1 and ΔG_2 are the effects of the R87G and D21E single mutations, respectively, and ΔG_{1+2} is the effect of the D21E + R87G double mutation on the parameters of the wild-type enzyme. For V_{max}, free energies of activation ($\Delta G^{\ddagger}$) are meant. [b] $\Delta G_{1+2} - \Delta G_1$. [c] $\Delta G_{1+2} - \Delta G_1 - \Delta G_2$.

categories may be distinguished by comparing $\Delta\Delta G_B$ with $-\Delta G_2$ (Table V).

Previous studies of the effects of second mutations on the kinetic properties of enzymes have found either no additional effect, partial additivity, additivity, or antagonism by the second mutation on the effects of the first (Carter et al., 1984; Knowles, 1987; Carter & Wells, 1988; Kuliopulos et al., 1990a,b; Blacklow & Knowles, 1990). With staphylococcal nuclease, when both kinetic and binding parameters of single and double mutants are studied, as summarized in Table VI, depending on which parameter is studied, the D21E + R87G double mutant shows differing quantitative interaction of the effects of the same pair of single mutations.

The simplest quantitative effect of a double mutation is additivity of the damaging effects of the single mutants on the free energy of an interaction. Such simple additivity is seen with the dissociation constants K_S and K_3 of the substrate 5′-pdTdA from the binary enzyme–substrate complex and from the ternary enzyme–metal–substrate complexes, respectively (Table VI). Both the R87G and D21E single mutations weaken substrate binding, and the double mutant shows the product of these weakening effects (Table VI). Such behavior is most simply explained by the independent binding of different portions of the substrate pdTdA by Arg-87 and by Asp-21 or by Ca^{2+}, which is held by Asp-21. The loss or alteration of either residue independently raises the free energy of substrate interactions in the ternary complex and these increases in ΔG are additive in the double mutant. Binding of the inhibitory metal Mn^{2+}, but not of the activating metal Ca^{2+}, in the ternary enzyme–metal–pdTp complex may also show simple additivity of effects on ΔG in the double mutant, presumably for analogous reasons.[3]

With the enzyme ketosteroid isomerase, simple additive, inhibitory effects on V_{max} of mutating the catalytic residues Tyr-14 and Asp-38 were observed in the double mutant Y14F + D38N (Kuliopulos et al., 1990a,b), and kinetic isotope effects with the wild-type isomerase showed that these two residues acted concertedly, i.e., in the same rate-limiting chemical step, to promote enolization of the substrate (Xue et al., 1990). In the present case, with Staphylococcal nuclease, the effects of the two active-site mutations on V_{max} are clearly antagonistic, since the double mutant, D21E + R87G, is 5-fold more active than R87G and $10^{3.7}$-fold more active than predicted by the product of the activity losses of the individual single mutants. In other words, as measured by $\Delta\Delta G_A^{\ddagger}$, the D21E mutation has partially suppressed the effect of the R87G mutation on V_{max} by −0.9 kcal/mol, and, as measured by $\Delta\Delta G_B^{\ddagger}$, the two mutations mutually antagonize each other's effect on V_{max} of the wild-type enzyme by −5.0 kcal/mol (Table VI).

The possibility of a stepwise mechanism in which Asp-21 and Arg-87 operate consecutively rather than concertedly in catalysis, leading to nonadditivity of the kinetic effects of the two mutations on V_{max}, was investigated by using ^{31}P NMR to search for the buildup of a trigonal-bipyramidal phosphorane intermediate with the R87G mutant. No evidence for an enzyme-bound phosphorane intermediate (<1% of the enzyme under steady-state conditions) was found, suggesting that this species is a transition state in a concerted process rather than a long-lived intermediate. Hence a reasonable alternative explanation for the −0.9 kcal/mol antagonistic kinetic effect of the D21E mutation on the R87G mutation in the double mutant is antagonistic structural effects of the two mutations on either the ground state or transition state of the enzyme-bound substrate. The dissociation constants of Ca^{2+} and of Mn^{2+} from the binary enzyme–metal complex (Table II) and the dissociation constants of Ca^{2+} from the ternary enzyme–metal–substrate complex (Table VI) also show such antagonistic behavior. Thus, as measured by $\Delta\Delta G_A$, the D21E mutation suppressed, by −0.5 to −1.1 kcal/mol, the weakening of metal binding produced by the R87G mutation, and, in the active ternary enzyme–Ca^{2+}–5′-pdTdA complex, a −1.0 kcal/mol antagonistic effect on Ca^{2+} binding is observed (Table VI), similar in magnitude to the $\Delta\Delta G_A^{\ddagger}$ value of −0.9 kcal/mol found for V_{max}, suggesting that the antagonistic kinetic effect results from a change at the Ca^{2+} binding site. Since Ca^{2+} is believed to coordinate both substrates of the staphylococcal nuclease reaction, the phosphodiester group and the attacking water molecule (Figure 1), changes in the position of Ca^{2+} with respect to its ligand Asp-21 and Arg-87 might profoundly alter both enzymatic activity and affinity for the metal ion. The large differences between $\Delta\Delta G_B^{\ddagger}$ for V_{max} (−5.0 kcal/mol) and $\Delta\Delta G_B$ for metal binding (−0.5 to −1.6 kcal/mol) indicate greater mutually antagonistic structural effects of the two mutations on the transition state than on the ground state of the active ternary complex (Table VI).

In three cases, no additional effect of the D21E mutation was found in the double mutant beyond that of the R87G single mutation (Table VI).[3] Such an absence of effect of the second mutation may represent a limiting case of an antagonistic structural effect, which coincidentally cancels the 0.6–0.7 kcal/mol further weakening expected from the D21E mutation. This seems likely for the dissociation constant K_A' of Ca^{2+} from the ternary pdTp complex and of Mn^{2+} from the ternary pdTdA complex, since clearly antagonic effects on Ca^{2+} and Mn^{2+} binding are found with other complexes of the double mutant.

Alternatively, no additional effect, as well as partial additivity of the effect of a second mutation in a double mutant, may result from the cooperative binding of differing portions of a ligand in the wild-type enzyme. Each single mutant shows extra weakening of ligand binding due to the loss of both a binding interaction and cooperativity. The double mutant loses two binding interactions but loses cooperativity only once, resulting in an overall weakening effect less than the product of the weakening effects of each single mutant. In such a case, $\Delta\Delta G_B$ measures the cooperativity of ligand binding. For example the $\Delta\Delta G_B$ value of −1.1 kcal/mol for K_2(Ca,pdTdA) may reflect the additional stabilization due to the cooperative binding of the Ca^{2+}–pdTdA complex by both Asp-21 and Arg-87 in the wild-type enzyme. This behavior differs from the binding of pdTdA alone, which shows simple additive effects of the two mutations, reflecting independent binding by the two residues (Table VI).

Synergistic effects of the two mutations are found on the binding of the substrate analogue pdTp both in the binary enzyme–pdTp and ternary enzyme–metal–pdTp complexes (Table VI). While such effects alone could be explained by extensive protein denaturation in the double mutant, this is unlikely, since metal binding remained nearly intact, simple additivity of damage was noted in substrate binding, and enzymatic activity increased above that of the R87G single mutation. An alternative explanation for the synergistic effects of the two mutations on the binding of pdTp might be strain or anticooperativity in the binding of two portions of the inhibitor by the wild-type enzyme. Each single mutation would then appear less damaging to binding, since, in addition to a lost interaction, negative cooperativity or strain would also have been lost in each case, resulting in a stronger residual interaction with the other residue. In the double mutant, both binding interactions are lost, but strain is lost only once, resulting in extra weakening of ligand binding beyond that predicted by the product of the effects of the single mutations. In such a case the positive value of $\Delta\Delta G_B$ measures the amount of strain in ligand binding by the wild-type enzyme, which is ~4 kcal/mol for pdTp binding and lower (2.8 kcal/mol) for Ca^{2+}–pdTp binding (Table VI).

Strain in the binding of pdTp by the wild-type enzyme may result from electrostatic repulsion between the 3′- and 5′-phosphates that are held near each other in the ternary enzyme–metal–pdTp complex (Serpersu et al., 1988). When the interaction with Arg-87 is abolished in the R87G single mutation, the two phosphates may separate, relieving strain and strengthening the interaction of pdTp with Ca^{2+}. A similar separation of phosphates might occur in the D21E single mutation due to a change in the position of Ca^{2+}, strengthening the interaction of pdTp with Arg-87. In the double mutant, when both interactions are abolished or altered, a much larger effect on the dissociation constant of pdTp is detected. Hence double mutations are sometimes necessary to detect enzyme–ligand interactions that are obscured by internal negative cooperativity.

It is clear from these studies that the quantitative effects of a double mutation are complicated and vary depending on the parameters studied. When two mutations interact in the same way on several parameters, a common underlying mechanism is suggested. By comparing the antagonistic effects of two mutations on catalysis by staphylococcal nuclease with their effects on the binding of metal activators, substrates, and

[3] Note that the category for K_A'(Mn,pdTp) is either "additive" or "no additional effect", since the 1.5-fold increase in K_A'(Mn,pdTp) in the D21E mutant is close to unity.

inhibitors, we find that the kinetic effects are best mimicked by the effects on Ca^{2+} binding, which are also antagonistic, by approximately the same factor. We conclude that the antagonistic effects on catalysis result from antagonistic structural effects at or near the Ca^{2+} binding site.

ACKNOWLEDGMENTS

We are grateful to Gregory P. Mullen for help with the ^{31}P NMR experiments, to William P. Jencks for cogent advice on the interactions of the effects of mutations, to Eaton E. Lattman and Athan Kuliopulos for helpful discussions, and to Peggy Ford for typing the manuscript.

REFERENCES

Anfinsen, C. B., Cuatrecasas, P., & Taniuchi, H. (1971) *Enzymes (3rd Ed.) 4*, 177–204.

Blacklow, S. C., & Knowles, J. R. (1990) *Biochemistry 29*, 4099–4108.

Carr, H. Y., & Purcell, E. M. (1954) *Phys. Rev. 94*, 630–638.

Carter, P., & Wells, J. A. (1988) *Nature 332*, 564–568.

Carter, P. J., Winter, G., Wilkinson, A. J., & Fersht, A. R. (1984) *Cell 38*, 835–840.

Chaiken, I. M., & Sanchez, G. R. (1972) *J. Biol. Chem. 247*, 6743–6747.

Cohn, M., & Towsend, J. (1954) *Nature 173*, 1090–1091.

Cotton, F. A., Hazen, E. E., Jr., & Legg, M. J. (1979) *Proc. Natl. Acad. Sci. U.S.A. 76*, 2551–2555.

Cuatrecasas, P., Fuchs, S., & Anfinsen, C. B. (1967a) *J. Biol. Chem. 242*, 1541–1547.

Cuatrecasas, P., Fuchs, S., & Anfinsen, C. B. (1967b) *J. Biol. Chem. 242*, 4759–4767.

Dunn, B. M., DiBello, C., & Anfinsen, C. B. (1973) *J. Biol. Chem. 248*, 4769–4774.

Hibler, D. W., Stolowich, J. N., Reynolds, M. A., Gerlt, J. A., Wilde, J. A., & Bolton, P. H. (1987) *Biochemistry 26*, 6278–6286.

Knowles, J. R. (1987) *Science 236*, 1252–1258.

Kuliopulos, A., Talalay, P., & Mildvan, A. S. (1990a) *Biophys. J. 57*, 39a.

Kuliopulos, A., Talalay, P., & Mildvan, A. S. (1990b) *Biochemistry* (in press).

Kumamoto, J., Cox, J. R., & Westheimer, F. H. (1956) *J. Am. Chem. Soc. 77*, 4858–4860.

Kunkel, T. A., Roberts, J. D., & Zakour, R. A. (1987) *Methods Enzymol. 154*, 367–383.

Lachica, R. V. F., Genegeorgis, C., & Hoeprich, P. O. (1971) *Appl. Microbiol. 21*, 585–587.

Loll, P. J., & Lattman, E. E. (1989) *Proteins 5*, 183–201.

Mildvan, A. S., & Cohn, M. (1963) *Biochemistry 2*, 910–919.

Mildvan, A. S., & Cohn, M. (1966) *J. Biol. Chem. 241*, 1178–1193.

Mildvan, A. S., & Engle, J. L. (1972) *Methods Enzymol. 49G*, 322–359.

Mildvan, A. S., & Fry, D. C. (1987) *Adv. Enzymol. Relat. Areas Mol. Biol. 59*, 241–313.

Reed, G. H., & Cohn, M. (1970) *J. Biol. Chem. 245*, 6539–6546.

Serpersu, E. H., Shortle, D., & Mildvan, A. S. (1986) *Biochemistry 25*, 68–77.

Serpersu, E. H., Shortle, D., & Mildvan, A. S. (1987) *Biochemistry 26*, 1289–1300.

Serpersu, E. H., McCracken, J., Peisach, J., & Mildvan, A. S. (1988a) *Biochemistry 27*, 8034–8044.

Serpersu, E. H., Shortle, D., & Mildvan, A. S. (1988b) *J. Cell Biol. 107*, 830a.

Serpersu, E. H., Hibler, D. W., Gerlt, J. A., & Mildvan, A. S. (1989) *Biochemistry 28*, 1539–1548.

Shortle, D. (1983) *Gene 22*, 181–189.

Shortle, D. (1986) *Protein Engineering, Applications in Science, Medicine and Industry*, pp 233–241, Academic Press, Inc., New York.

Shortle, D., & Lin, B. (1985) *Genetics 110*, 539–555.

Tabor, S., & Richardson, C. C. (1987) *Proc. Natl. Acad. Sci. U.S.A. 84*, 4767–4771.

Tucker, P. W., Hazen, E. E., Jr., & Cotton, F. A. (1978) *Mol. Cell. Biochem. 22*, 67–77.

Tucker, P. W., Hazen, E. E., Jr., & Cotton, F. A. (1979) *Mol. Cell. Biochem. 23*, 67–86.

Weber, D. J., Lebowitz, M. S., & Mildvan, A. S. (1990a) *FASEB J. 4*, 1659a (Abstracts of the ASBMB/AAI Meeting, New Orleans).

Weber, D. J., Serpersu, E. H., & Mildvan, A. S. (1990b) *Biophys. J. 57*, 39a.

Xue, L., Talalay, P., & Mildvan. A. S. (1990) *Biochemistry 29*, 2203.